Eur Radiol (2015) 25:3499–3507
DOI 10.1007/s00330-015-3783-3

MUSCULOSKELETAL

Whole-body MRI in adult inflammatory myopathies: Do we need imaging of the trunk?

Lukas Filli[1] · Britta Maurer[2] · Andrei Manoliu[1] · Gustav Andreisek[1] · Roman Guggenberger[1]

Received: 10 November 2014 / Revised: 30 March 2015 / Accepted: 8 April 2015 / Published online: 24 April 2015

Abstract
Objective To evaluate whether imaging of the trunk could be omitted in patients with inflammatory myopathies without losing diagnostic accuracy using a restricted whole-body magnetic resonance imaging (rWB-MRI) protocol.
Methods After approval by the institutional review board, this study was performed in 63 patients (male/female, 13/50; median age, 52 years; range, 20–81 years) with new-onset myopathic symptoms (group 1, n=41) or previously diagnosed inflammatory myopathy (group 2, n=22). After performing whole-body MRI (WB-MRI) at 3.0 Tesla, myositis and fatty atrophy were evaluated in different muscles by two independent radiologists. The intra-class correlation coefficient (ICC) was calculated to evaluate inter-observer reliability.
Results Acquisition time was 56:01 minutes for WB-MRI and 37:37 minutes (32.8 % shorter) for rWB-MRI. In group 1, 14 patients were diagnosed with inflammatory myopathy based on muscle biopsy. rWB-MRI and WB-MRI showed equal sensitivity (42.9 %) and specificity (100 %) for myositis, and showed equal sensitivity (71.4 %) and similar specificity (63.0 % and 48.1 %, respectively) for fatty atrophy. No myositis was found in the body trunk in any patient. Inter-observer reliability was between substantial and perfect (ICC, 0.77–1.00).
Conclusions rWB-MRI showed diagnostic accuracy similar to WB-MRI for inflammatory myopathy at markedly reduced overall acquisition time.
Key Points
- *Whole-body MRI (WB-MRI) is a time-consuming imaging modality.*
- *A shortened MRI protocol was evaluated for inflammatory myopathies.*
- *The proposed protocol showed diagnostic accuracy similar to WB-MRI.*

Keywords Magnetic resonance imaging · Whole-body · Inflammatory myopathy · Polymyositis · Dermatomyositis

✉ Lukas Filli
lukas.filli@usz.ch

Britta Maurer
britta.maurer@usz.ch

Andrei Manoliu
andrei.manoliu@usz.ch

Gustav Andreisek
gustav@andreisek.de

Roman Guggenberger
roman.guggenberger@usz.ch

[1] Institute of Diagnostic and Interventional Radiology, University Hospital Zurich, University of Zurich, Raemistrasse 100, 8091 Zurich, Switzerland

[2] Division of Rheumatology, University Hospital Zurich, University of Zurich, Gloriastrasse 25, 8091 Zurich, Switzerland

Introduction

Magnetic resonance imaging (MRI) is a widely used imaging modality for the diagnosis and follow-up of muscle changes in inflammatory myopathies [1–7], which mainly include polymyositis and dermatomyositis with specific clinic-serologic subtypes. Traditionally, MRI focused on selected muscle regions depending on clinically suspected muscle changes [8, 9]. In the past few years, however, the use of whole-body MRI (WB-MRI) has been increasingly propagated because of its several advantages. For example, this technique allows additional detection of affected yet clinically "silent" muscle groups, especially in early disease when muscle strength is still preserved. Furthermore, the recognition of spatial distribution patterns of muscle involvement—most often

symmetrical yet multifocal—helps to differentiate inflammatory from neurodegenerative muscle disease and can guide muscle biopsy, with a substantial improvement in diagnostic accuracy (without MRI, the false-negative biopsy rate has been found to be up to 45 %) [10]. In patients with an established diagnosis, WB-MRI helps to distinguish muscle weakness due to persistent inflammation as opposed to fatty atrophy, and thus substantially influences therapeutic decisions.

Current MRI protocols usually include both T1-weighted and short-tau inversion recovery (STIR) sequences in order to assess fatty atrophy and depict muscle oedema, respectively [1, 2]. Despite technical advances such as parallel imaging and free table movement [11], WB-MRI remains time-consuming, and thus uncomfortable for patients. Total imaging time is typically around 45 minutes [1, 2, 12], and even longer in the case of additional contrast-enhanced sequences [2, 13].

There is a general consensus among clinical experts in the field that in adult patients with myositis, the body trunk is rarely involved [14, 15]. Hence, we hypothesized that imaging of the trunk could be dropped, favouring a time-saving restricted WB-MRI (rWB-MRI) protocol confined to the muscles of the upper and lower extremities. The purpose of this study was to evaluate whether imaging of the trunk could be omitted using an rWB-MRI protocol without losing accuracy in the diagnosis of inflammatory myopathy.

Materials and methods

Study subjects

After approval by the institutional review board, this prospective study was performed in 63 consecutive adult patients (male/female, 13/50; median age, 52 years; range, 20–81 years) who were seen in the rheumatology division and referred to the department of radiology for WB-MRI between December 2012 and February 2014. Patients presented either with new-onset myopathic symptoms, e.g. myalgia, muscle fatigue, reduced muscle strength or endurance (group 1, n=41; male/female, 11/30; median age, 52 years; range, 20–81 years), or for follow-up visits of established inflammatory myopathy (group 2, n=22; male/female, 2/20; median age, 53 years; range, 21–77 years). All patients underwent comprehensive diagnostic workup including clinical assessment, laboratory studies and muscle biopsy. For the purpose of this study, group 1 was further subdivided into patients who later were (group 1A) or were not (group 1B) diagnosed with inflammatory myopathy.

Whole-body MRI

All WB-MRI examinations were performed on a standard 3.0T MR scanner (Magnetom Skyra; Siemens Healthcare, Erlangen, Germany) using the complete whole-body matrix coil set (including a 20-channel head/neck coil, a 32-channel spine coil, two 18-channel body coils and a 36-channel peripheral coil). Patients were positioned in supine position. The standard whole-body imaging protocol included six stacks of STIR sequences in coronal plane (neck, chest, abdomen, pelvis, upper and lower legs; chest and abdomen with respiratory triggering; TR, 3,500–6,000 ms; TE, 257–353 ms; slice thickness, 4 mm; slice gap, 0 mm; in-plane resolution, 1.5×1.1 mm^2; number of averages, 2) as well as six stacks of axial pre- and post-contrast T1-weighted turbo spin-echo (TSE) sequences (TR, 702 ms; TE, 8.7 ms in-phase and 11 ms opposed-phase; slice thickness, 4 mm; slice gap, 5 mm; in-plane resolution, 1.4×1.4 mm^2; number of averages, 2). The TSE sequences were acquired using the Dixon technique, which allowed calculating water-only and fat-only images out of the in-phase and opposed phase images. The overall field of view was 180 (longitudinal)×50 (transversal)×40 cm (sagittal). The total acquisition time for the full whole-body protocol (WB-MRI) was 56 min, 1 s. Dropping the stacks for the body trunk (chest and abdomen) reduced the acquisition time by 18 min, 24 s (32.8 %), resulting in a remaining acquisition time of only 37 min, 37 s.

Image analysis

For all subjects, key muscles (as defined below) were assessed in terms of myositis and fatty atrophy by two independent musculoskeletal radiologists (L.F., and A.M., further referred to as reader 1 [R1] and reader 2 [R2]), who were blinded to clinical data and laboratory values. Subsequently, a common readout was performed on muscles scored differently by the two readers in order to reach consensus. Active myositis was defined as hyperintense signal abnormality in the muscles on STIR or water-only images (muscle oedema) with corresponding enhancement on post-contrast fat-suppressed T1-weighted images. Similar to a previous study [3], active myositis was scored 0 (none), 1 (focal) or 2 (involving>50 % of the muscle) in each muscle. Fatty atrophy was also evaluated in each muscle on the in-phase TSE and fat-only images according to the Goutallier classification [16]: 0 (normal, no fatty streak), 1 (some fatty streaks), 2 (important fatty streaks, but still more muscle than fat), 3 (as much fat as muscle), or 4 (more fat than muscle). Example images of myositis and fatty atrophy are provided in Fig. 1.

The total myositis and fatty atrophy scores (i.e. the respective sums of all values) were then calculated as follows: Scores for rWB-MRI included the deltoid, rotator cuff, biceps, triceps, gluteus, quadriceps, adductor, hamstring, and tibialis

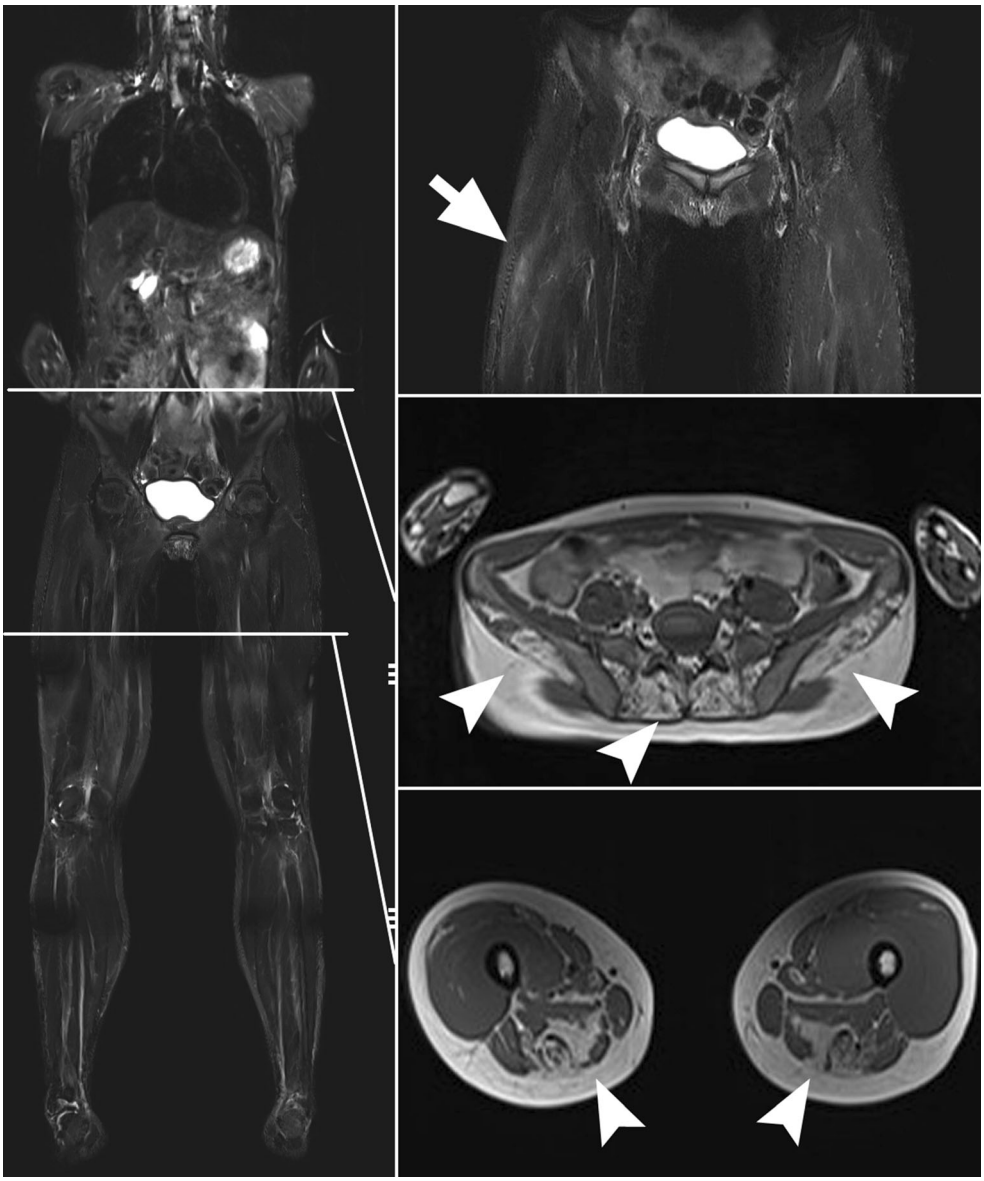

Fig. 1 Whole-body MR images of a 35-year-old female patient diagnosed with polymyositis 5 months prior and treated with prednisone and methotrexate (included in group 2). No muscle abnormalities were present in the body trunk. *Left:* Coronal whole-body STIR image automatically generated from six separate stacks. *Right: Top:* Coronal STIR image showing oedema (*arrow*) in the quadriceps muscle on the right side. *Middle and bottom:* Axial TSE images (in-phase) illustrating bilateral fatty atrophy (*arrowheads*) in the gluteus medius, erector spinae and hamstring muscles

anterior muscles. Scores for WB-MRI also included muscles of the body trunk, namely the pectorales, trapezius, serratus anterior, latissimus dorsi, intercostales, erector spinae, abdominal wall, and iliopsoas muscles. Small muscles such as the neck flexors or muscles in the forearm and feet were not included due to limited image resolution and/or field-of-view coverage.

In addition to the muscle scores, incidental findings in other organs of the body trunk were assessed by both radiologists during the consensus reading.

Statistical analysis

All statistical analysis was performed using SPSS software (version 20; IBM Corp., Armonk, NY, USA). Demographic data, clinical parameters and muscle scores of the different groups were compared using multivariate analysis of variance (ANOVA) and post hoc analysis with Fisher's least significant difference (LSD) test; a p value of <0.05 indicated significant differences.

Inter-observer agreement was evaluated by calculating intra-class correlation coefficients (ICCs). An ICC value of 0.21–0.40 was interpreted as fair agreement, 0.41–0.60 as moderate agreement, 0.61–0.80 as good agreement, 0.81–0.99 as almost perfect agreement, and 1.00 as perfect agreement [17].

Total myositis and fatty atrophy scores for the different groups were compared between rWB-MRI and WB-MRI using Student's paired t tests with Bonferroni correction.

For groups 1A (inflammatory myopathy) and 1B (no inflammatory myopathy, i.e. negative controls), sensitivity and specificity of the myositis and fatty atrophy scores were

calculated in both WB-MRI and rWB-MRI based on the final consensus readout. The area under the receiver operating characteristic (ROC) curve was calculated to evaluate the diagnostic accuracy of the respective scores. An area under the curve of 0.70–0.79 was considered to indicate a fair test and 0.51–0.69 was considered to indicate a poor test for discriminating between patients with and without inflammatory myopathy [18]. For group 2, WB-MRI and rWB-MRI were compared in terms of the myositis and fatty atrophy scores only; sensitivity and specificity were not calculated, since these patients were already diagnosed with and treated for inflammatory myopathy.

Since fatty atrophy of the erector spinae muscle was a common finding in all groups (*see* below), its correlation with age and time since diagnosis was assessed by calculating Kendall's correlation coefficient (τ).

Results

Demographical and clinical data

Of the 41 patients with new-onset myopathic symptoms (group 1), 14 were subsequently diagnosed with inflammatory myopathy (group 1A), whereas no inflammatory myopathy was diagnosed in the other 27 patients (group 1B). The patients in group 2 had been previously diagnosed with inflammatory myopathy and received follow-up imaging for control of treatment response.

No significant differences with regard to age, creatinine phosphokinase (CPK), C-reactive protein (CRP) or lactate dehydrogenase (LDH) were found among the three patient groups (group 1A vs. group 1B: p values 0.06–0.35; group 1A vs. group 2: p-values 0.32–0.93; group 1B vs. group 2: p values 0.10–0.39). The CPK was markedly elevated (1,418 IU/L, normal<167 IU/L) in one outlier patient in group 2 with severe immune-mediated necrotizing myositis, which is a common and typical phenomenon in those patients; the CPK in the other patients of group 2 was in the range of 33–535 IU/L (Table 1).

Comparison of muscle scores among patient groups

Inter-observer reliability was "almost perfect" to "perfect" for myositis (ICC, 0.89–1.00) and "substantial" to "almost perfect" for fatty atrophy (ICC, 0.77–0.97). Table 2 provides the respective values of total myositis and fatty atrophy scores for WB-MRI and rWB-MRI. In both WB-MRI and rWB-MRI, the myositis score was significantly higher in group 1A than group 1B (WB-MRI: $p<0.001$; rWB-MRI: $p<0.001$). Furthermore, the myositis score was higher in group 2 than group 1A (WB-MRI: $p=0.026$; rWB-MRI: $p=0.025$) and 1B (WB-MRI: $p=0.001$; rWB-MRI: $p=0.001$). Group 1B showed the

Table 1 Demographics and relevant clinical data of the different patient groups

	Group 1A ($n=14$)	Group 1B ($n=27$)	Group 2 ($n=22$)
Diagnosis	PM ($n=8$), DM ($n=4$), myositis associated with Sjögren's syndrome ($n=1$), overlap syndrome ($n=1$)	No inflammatory myopathy ($n=27$)	PM ($n=9$), DM ($n=4$), JDM ($n=1$), myositis associated with SSc ($n=4$), myositis associated with Sjögren's syndrome ($n=2$), overlap syndrome ($n=2$)
Disease duration at time of MRI (weeks), median (range)	1 week (0–3)	1.5 weeks (0–3)	80 weeks (20–720)
Age (years), median (range)	68 (22–81)	46.5 (20–80)	53 (21–77)
CPK (IU/l, normal<167), median (range)	103 (47–365)	177 (39–1,572)	92 (33–1,418)
CRP (mg/l, < 5), median (range)	1.0 (0.4–15)	1.8 (0.3–4.4)	4.7 (0.3–35.0)
LDH (IU/l, 240–480), median (range)	337 (268–680)	372 (219–601)	385 (265–568)
MMT8, median (range)	64.5 (60–80)	65 (44–80)	59 (46–73)
FI-2: shoulder flexion, shoulder abduction, head lift, hip flexion, step test, heel lift, toe lift), % of maximum, median (range)	47 (20–70), 52 (27–100), 37 (15–55), 43 (12–58), 38 (27–60), 35.5 (28–71), 33 (9–46)	95 (12.5–100), 100 (25–100), 47.5 (15–100), 68 (28–100), 100 (50–100), 69 (38–100), 96 (12–100)	20 (12–100), 33 (10–100), 25 (8–100), 27 (10–100), 27 (8–100), 19 (13–100), 28 (13–100)
Anti-inflammatory and disease-modifying anti-rheumatic drugs	Prednisone ($n=10$), prednisone+MTX ($n=4$)	-	Prednisone+MTX ($n=7$), prednisone+AZT ($n=4$), MTX ($n=4$), AZT ($n=2$), none ($n=5$)

PM polymyositis, *DM* dermatomyositis, *JDM* juvenile dermatomyositis, *SSc* systemic sclerosis, *CPK* creatinine phosphokinase, *CRP* C-reactive protein, *LDH* lactate dehydrogenase, *MRI* magnetic resonance imaging, *MTX* methotrexate, *AZT* azathioprine, *MMT8* manual muscle testing score, *FI-2* myositis functional index-2

Table 2 Mean values±standard deviation of total myositis and fatty atrophy scores of whole-body magnetic resonance imaging (WB-MRI) and restricted WB-MRI (rWB-MRI) readouts performed by two radiologists independently and in consensus

		WB-MRI			rWB-MRI		
		Group 1A	Group 1B	Group 2	Group 1A	Group 1B	Group 2
Myositis	R1	1.8±2.1	0.0±0.0	2.6±4.5	1.8±2.1	0.0±0.0	2.6±4.5
	R2	1.4±2.1	0.0±0.0	2.5±4.3	1.4±2.1	0.0±0.0	2.5±4.3
	Inter-observer reliability	ICC=0.89 (p<0.001)	ICC=1.00 (p<0.001)	ICC=0.94 (p<0.001)	ICC=0.89 (p<0.001)	ICC=1.00 (p<0.001)	ICC=0.94 (p<0.001)
	Consensus	1.6±2.2	0.0±0.0	2.6±4.5	1.6±2.2	0.0±0.0	2.6±4.5
Fatty atrophy	R1	5.7±5.2	8.5±17.4	6.2±6.9	4.3±4.2	6.2±12.5	3.9±5.3
	R2	5.8±5.3	9.2±16.2	6.0±7.0	5.0±4.2	5.9±11.2	4.1±5.0
	Inter-observer reliability	ICC=0.77 (p<0.001)	ICC=0.93 (p<0.001)	ICC=0.92 (p<0.001)	ICC=0.81 (p<0.001)	ICC=0.97 (p<0.001)	ICC=0.9 (p<0.001)
	Consensus	5.7±5.2	8.5±17.0	6.2±6.9	4.3±4.2	6.1±12.0	4.1±5.2

ICC intra-class correlation coefficient, *R1/R2* reader 1 and reader 2

highest fatty atrophy scores; however, there was no significant difference in scores among the groups (WB-MRI: p values= 0.22-0.92; rWB-MRI: p values=0.17-0.44).

In both groups 1A and 2, the quadriceps muscles showed the highest myositis scores (0.57±0.62 and 0.55±0.78, respectively), underscoring the predominant affection of proximal muscles, especially of the lower extremities. Patients with new-onset inflammatory myopathy showed myositis mainly in the quadriceps muscles, whereas those with established disease and longer disease duration also showed involvement of the pelvic girdle. No myositis was found in the muscles of the body trunk in any patient (Fig. 2).

The most common finding in the trunk in all patient groups was fatty atrophy of the erector spinae muscle at the lumbar level, which was present in 40 patients (63.5 %), with a resulting score for muscle atrophy of 0.98±0.99 (mean±standard deviation). This finding, which is commonly related to age-related degeneration and hyperlordosis [19, 20], was not significantly higher in any patient group compared to the other groups (p -values=0.31–0.58); it showed a weakly positive correlation with age (Kendall's correlation coefficient τ, 0.33, p=0.02), but no significant correlation with time since diagnosis or since initial presentation (τ -0.01, p=0.96). Patients in group 2 who did not receive drug treatment (n=5) showed only mild fatty atrophy of the lumbar erector spinae muscle.

WB-MRI vs. rWB-MRI

Because no myositis was found in the body trunk of any patient, the total myositis scores in WB-MRI and rWB-MRI were equal. The total fatty atrophy scores were significantly higher in WB-MRI than rWB-MRI in all groups (group 1A, p=0.005; group 1B, p=0.009; group 2. p<0.001), which is largely explained by the frequent involvement of the erector spinae muscle (*see* above) (Fig. 2).

The performance of rWB-MRI and WB-MRI for the diagnosis of myositis in our population was identical (sensitivity, 42.9 %; specificity 100 %; positive predictive value, 100 %; negative predictive value, 77.1 %). For fatty atrophy, the sensitivity was equal in rWB-MRI and WB-MRI (71.4 % and 71.4 %, respectively), but the specificity was even higher in rWB-MRI than WB-MRI (63.0 % vs. 48.1 %, respectively). The area under the ROC curve of the myositis score was equal in both rWB-MRI and WB-MRI (0.714) and, according to the aforementioned interpretation, indicated "fair" test accuracy. The area under the ROC curve for fatty atrophy score was 0.598 for WB-MRI and 0.672 for rWB-MRI, corresponding to "poor" test accuracy. This means that the myositis score allowed "fair" discrimination between patients with and without inflammatory myopathy,

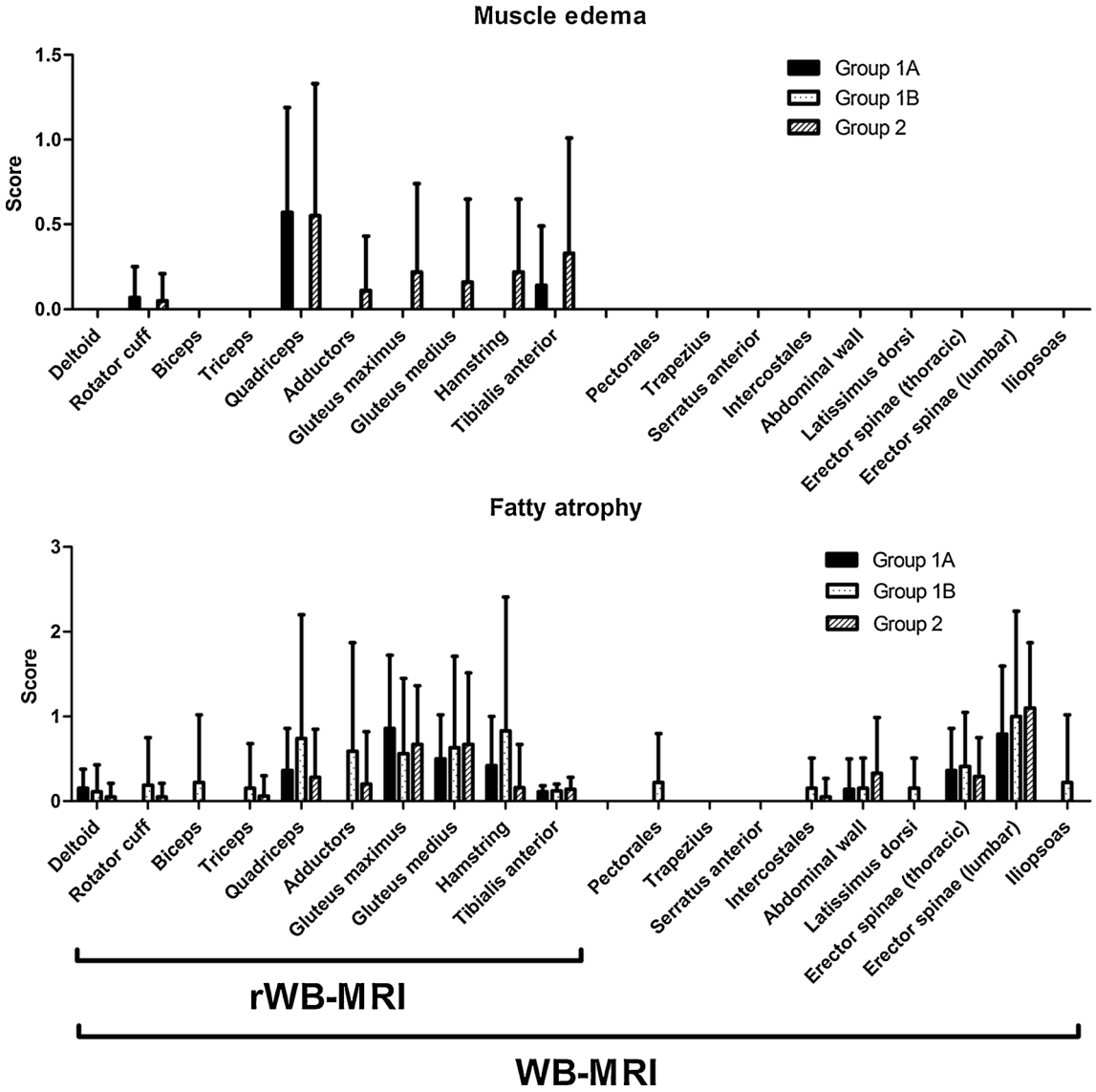

Fig. 2 Myositis (range 0–2) and fatty atrophy (range 0–4) in key muscles included in the whole-body magnetic resonance imaging (WB-MRI) and restricted WB-MRI (rWB-MRI) assessments, respectively, of the different patient groups (1A, 1B, 2). Data are presented as mean values (*bars*) with standard deviation (*whiskers*), and are obtained from the consensus readouts of two radiologists. For better visibility, data from the right and left side of the body are merged

whereas the fatty atrophy score allowed "poor" discrimination between them.

Incidental findings in the body trunk

Incidental findings in the chest included cardiomegaly (n=1), a vertebral hemangioma (n=1), multinodular goiter (n=2), and a cystic lesion in the posterior mediastinum (n=1), which was interpreted as a lymphogenic cyst on a dedicated chest CT 7 days later. In the abdomen, findings included single or multiple liver cysts (n=8), liver hemangiomas (n=3), renal cysts (n=12), diverticulosis of the sigmoid colon (n=5), gallstones (n=3), uterine fibroids (n=4) and cystic adnexal masses (n=6) (Fig. 3). One patient had a hip prosthesis, which did not affect muscle assessment.

Discussion

The present study compared diagnostic accuracy between a restricted WB-MRI (rWB-MRI) and a conventional WB-MRI protocol in adult patients with either clinically suspected or previously diagnosed inflammatory myopathy. Results showed that the accuracy of rWB-MRI was almost equal to that of conventional WB-MRI for the diagnosis of new-onset inflammatory myopathy or in follow-up examinations.

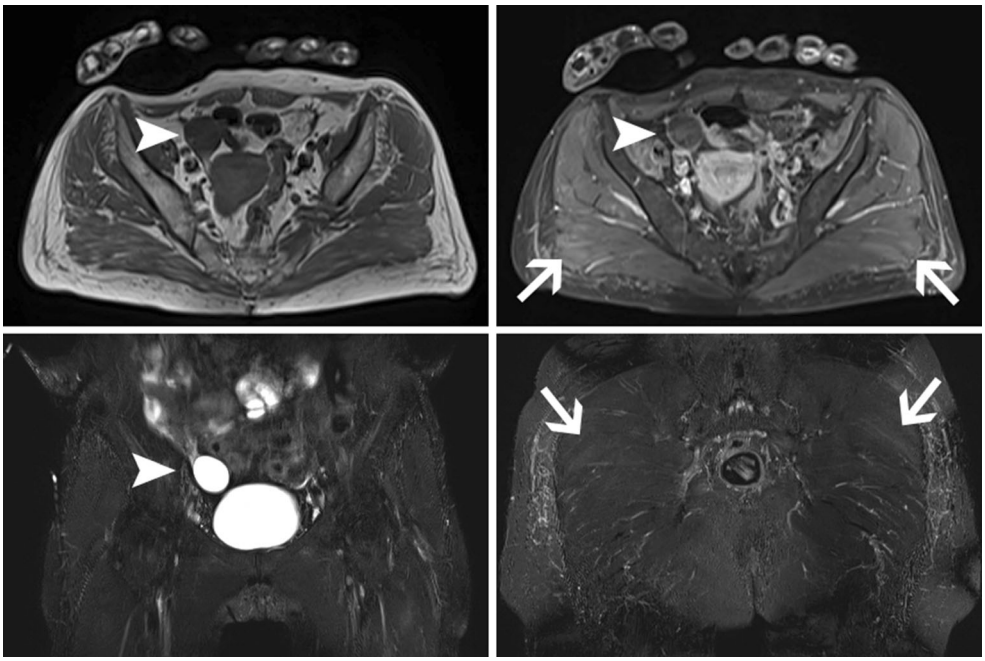

Fig. 3 Axial pre- (*top left*) and post-contrast (*top right*) T1-weighted images and coronal STIR images (*bottom*) of a 57-year old female patient from group 2 diagnosed with polymyositis. Note the subtle hyperintensities in the gluteus maximus muscles bilaterally on STIR, which are confirmed as inflammatory muscle oedema on contrast-enhanced images (*arrows*). Following contrast administration, the incidental finding of a right-sided cystic ovarian mass (*arrowheads*) could be classified as benign

Polymyositis, dermatomyositis and myopathy associated with systemic sclerosis typically involve the shoulder girdle and pelvic girdle, including the proximal extremities, and muscle changes are readily seen on WB-MRI [21, 22]. The observations in the present study agree with those in the literature: in new-onset inflammatory myopathy, the quadriceps muscles were most frequently involved, whereas in long-standing disease, other muscles of the proximal extremities were also involved. This additional involvement of other muscle groups explains the higher myositis score in patients with long-standing disease (group 2) compared to those with recent diagnosis (group 1A).

None of the assessed muscles of the body trunk in any of the patients were found to be affected by myositis. This finding confirms the rarity of involvement of the body trunk in patients with inflammatory myopathies [23]. In contrast to adult forms of inflammatory myopathies, juvenile dermatomyositis (JDM) has been reported to show a high prevalence of muscle changes in the abdominal wall (56 %) and psoas muscles (54 %) seen in WB-MRI [3]. Other rare systemic diseases that involve thoracic and abdominal muscles include muscle dystrophies, neuromuscular diseases, and glycogen storage diseases [21, 24–27]. However, these entities commonly present in childhood, where WB-MRI may be performed only under general anaesthesia. In addition, the role of WB-MRI in these disorders has yet to be clarified. Patients with inflammatory myopathies have a substantially increased risk for malignancies compared to the general population [28, 29]. Dermatomyositis is associated with lung, gastric, pancreatic, colorectal, and ovarian cancers [30], whereas polymyositis is associated with non-Hodgkin lymphoma, lung cancer and bladder cancer [30]. Cancer screening is usually performed with computed tomography of the chest and abdomen, gynaecological and urological examination, and blood analysis. There are no official guidelines recommending WB-MRI as a cancer screening tool in inflammatory myopathies, particularly not a protocol dedicated to the detection of myositis, which for example does not include diffusion-weighted imaging. No malignant disease was discovered in the present study. Even without abdominal imaging in an rWB-MRI protocol, the pelvic organs (and thus incidental findings such as adnexal masses) are still covered on the images of the pelvis (Fig. 3). Therefore, in our view, the purported higher incidence of malignancies in these patients does not preclude using an rWB-MRI protocol. Systemic muscle diseases, mainly polymyositis, frequently involve the heart muscle [31]; however, cardiac imaging requires a dedicated protocol, and the heart cannot be reliably assessed with current WB-MRI methods.

MRI has proven useful for detecting muscle changes and for differentiating acute inflammation (myositis) from chronic damage (fatty atrophy). MR protocols in suspected myopathy should include both STIR images to depict muscle oedema and T1-weighted images to assess fatty atrophy [1, 2]. Furthermore, images should be acquired in both axial and coronal orientation for the detection of heterogeneous and multifocal involvement within individual muscles [12, 27]. Imaging parameters of the WB-MRI protocol in the present study, including repetition time, echo time, and slice thickness, were comparable to those in other protocols reported in the literature [21, 32]. Our protocol also included contrast-enhanced axial TSE images, the benefit of which in inflammatory myopathies is controversial [2, 13]. In our WB-MRI protocol, almost the same amount of time could have been saved by renouncing

the contrast-enhanced images instead of using rWB-MRI (18:30 min and 18:24 min, respectively). However, we found them indispensable for confirmation of suspected muscle inflammation, to differentiate inflammatory myopathy from other forms of myopathy (such as neurodegenerative or metabolic disease), and for further characterization of incidental findings, e.g. cystic ovarian masses (Fig. 3).

Our study has several limitations. First, it is a retrospective study with an inherent bias regarding the inclusion of study subjects. The patients showed rather low myositis scores, which may be explained with the early time of diagnosis and/or therapeutic success. Given the low myositis scores, the ROC analyses should be interpreted with caution. In a larger, more general patient population, the performance of the myositis score may be different (e.g. higher) in both WB-MRI and rWB-MRI. Second, the observation period of this study does not principally rule out false-negative cases; however, to date, none of the patients in group 1B have been diagnosed with inflammatory myopathy. Lastly, the rWB-MRI protocol was virtually obtained by dropping the images of the chest and abdomen. A real rWB-MRI protocol, however, could have been optimized for image resolution or signal-to-noise ratio in the remaining stacks while maintaining some gain in time over a regular WB-MRI protocol. Thus the saved time could be used, at least in part, to improve other imaging aspects.

In conclusion, whole-body MRI restricted to the proximal extremities—with omission of the body trunk—shows similar accuracy for diagnosis and follow-up of patients with inflammatory myopathy.

Acknowledgments The scientific guarantor of this publication is Roman Guggenberger, MD. The authors of this manuscript declare no relationships with any companies whose products or services may be related to the subject matter of the article. The authors state that this work has not received any funding. No complex statistical methods were necessary for this paper. Institutional review board approval was obtained. Written informed consent was obtained from all subjects (patients) in this study. Methodology: prospective, diagnostic or prognostic study, performed at one institution.

References

1. Lenk S, Fischer S, Kotter I, Claussen CD, Schlemmer HP (2004) Possibilities of whole-body MRI for investigating musculoskeletal diseases. Radiologe 44:844–853
2. Schmidt GP, Reiser MF, Baur-Melnyk A (2007) Whole-body imaging of the musculoskeletal system: the value of MR imaging. Skelet Radiol 36:1109–1119
3. Malattia C, Damasio MB, Madeo A et al (2013) Whole-body MRI in the assessment of disease activity in juvenile dermatomyositis. Ann Rheum Dis. doi:10.1136/annrheumdis-2012-202915
4. Boutry N, Hachulla E, Zanetti-Musielak C, Morel M, Demondion X, Cotten A (2007) Imaging features of musculoskeletal involvement in systemic sclerosis. Eur Radiol 17:1172–1180
5. Mavrogeni S, Sfikakis PP, Dimitroulas T, Kolovou G, Kitas GD (2014) Cardiac and muscular involvement in idiopathic inflammatory myopathies: noninvasive diagnostic assessment and the role of cardiovascular and skeletal magnetic resonance imaging. Inflamm Allergy Drug Targets 13:206–216
6. Del Grande F, Carrino JA, Del Grande M, Mammen AL, Christopher Stine L (2011) Magnetic resonance imaging of inflammatory myopathies. Top Magn Reson Imaging 22:39–43
7. Castro TC, Lederman H, Terreri MT, Caldana WI, Zanoteli E, Hilario MO (2014) Whole-body magnetic resonance imaging in the assessment of muscular involvement in juvenile dermatomyositis/polymyositis patients. Scand J Rheumatol 43: 329–333
8. Garcia J (2000) MRI in inflammatory myopathies. Skelet Radiol 29:425–438
9. Fraser DD, Frank JA, Dalakas M, Miller FW, Hicks JE, Plotz P (1991) Magnetic resonance imaging in the idiopathic inflammatory myopathies. J Rheumatol 18:1693–1700
10. Connor A, Stebbings S, Anne Hung N, Hammond-Tooke G, Meikle G, Highton J (2007) STIR MRI to direct muscle biopsy in suspected idiopathic inflammatory myopathy. J Clin Rheumatol 13: 341–345
11. Zenge MO, Ladd ME, Quick HH (2009) Novel reconstruction method for three-dimensional axial continuously moving table whole-body magnetic resonance imaging featuring autocalibrated parallel imaging GRAPPA. Magn Reson Med 61:867–873
12. Weckbach S (2012) Whole-body MRI for inflammatory arthritis and other multifocal rheumatoid diseases. Semin Musculoskelet Radiol 16:377–388
13. Park JH, Olsen NJ (2001) Utility of magnetic resonance imaging in the evaluation of patients with inflammatory myopathies. Curr Rheumatol Rep 3:334–345
14. Harris-Love MO, Shrader JA, Koziol D et al (2009) Distribution and severity of weakness among patients with polymyositis, dermatomyositis and juvenile dermatomyositis. Rheumatology (Oxford) 48:134–139
15. Rider LG, Koziol D, Giannini EH et al (2010) Validation of manual muscle testing and a subset of eight muscles for adult and juvenile idiopathic inflammatory myopathies. Arthritis Care Res 62:465–472
16. Goutallier D, Postel JM, Bernageau J, Lavau L, Voisin MC (1994) Fatty muscle degeneration in cuff ruptures. Pre- and postoperative evaluation by CT scan. Clin Orthop Relat Res 304:78–83
17. Kundel HL, Polansky M (2003) Measurement of observer agreement. Radiology 228:303–308
18. Hanley JA, McNeil BJ (1982) The meaning and use of the area under a receiver operating characteristic (ROC) curve. Radiology 143:29–36
19. Parkkola R, Rytokoski U, Kormano M (1993) Magnetic resonance imaging of the discs and trunk muscles in patients with chronic low back pain and healthy control subjects. Spine (Phila Pa 1976) 18: 830–836
20. Pezolato A, de Vasconcelos EE, Defino HL, Nogueira-Barbosa MH (2012) Fat infiltration in the lumbar multifidus and erector spinae muscles in subjects with sway-back posture. Eur Spine J 21:2158–2164
21. Cantwell C, Ryan M, O'Connell M et al (2005) A comparison of inflammatory myopathies at whole-body turbo STIR MRI. Clin Radiol 60:261–267
22. Schanz S, Henes J, Ulmer A et al (2013) Magnetic resonance imaging findings in patients with systemic scleroderma and musculoskeletal symptoms. Eur Radiol 23:212–221
23. O'Connell MJ, Powell T, Brennan D, Lynch T, McCarthy CJ, Eustace SJ (2002) Whole-body MR imaging in the diagnosis of polymyositis. AJR Am J Roentgenol 179:967–971

24. Dalakas MC (2011) Review: an update on inflammatory and autoimmune myopathies. Neuropathol Appl Neurobiol 37:226–242
25. Dalakas MC (2010) Inflammatory muscle diseases: a critical review on pathogenesis and therapies. Curr Opin Pharmacol 10:346–352
26. Carlier RY, Laforet P, Wary C et al (2011) Whole-body muscle MRI in 20 patients suffering from late onset Pompe disease: involvement patterns. Neuromuscul Disord 21:791–799
27. Quijano-Roy S, Avila-Smirnow D, Carlier RY (2012) Whole body muscle MRI protocol: pattern recognition in early onset NM disorders. Neuromuscul Disord 22:S68–S84
28. Baer AN (2011) Paraneoplastic muscle disease. Rheum Dis Clin N Am 37:185–200, v-vi
29. Buchbinder R, Forbes A, Hall S, Dennett X, Giles G (2001) Incidence of malignant disease in biopsy-proven inflammatory myopathy. A population-based cohort study. Ann Intern Med 134: 1087–1095
30. Hill CL, Zhang Y, Sigurgeirsson B et al (2001) Frequency of specific cancer types in dermatomyositis and polymyositis: a population-based study. Lancet 357:96–100
31. Lundberg IE (2006) The heart in dermatomyositis and polymyositis. Rheumatology (Oxford) 45:iv18–iv21
32. Jarraya M, Quijano-Roy S, Monnier N et al (2012) Whole-body muscle MRI in a series of patients with congenital myopathy related to TPM2 gene mutations. Neuromuscul Disord 22:S137–S147